

# The Construction and Performance of the CsI Hodoscopic Calorimeter for the GLAST Beam Test Engineering Module<sup>1</sup>

W. Neil Johnson<sup>2</sup>, J. Eric Grove<sup>2</sup>, Bernard F. Philips<sup>3</sup>,  
James Ampe<sup>4</sup>, Satpal Singh<sup>5</sup>, and Eric Ponslet<sup>6</sup>

(Representing the GLAST LAT Collaboration)

<sup>2</sup>Naval Research Lab, Washington DC 20375

<sup>3</sup>George Mason University, Fairfax VA

<sup>4</sup>Praxis, Inc, Alexandria VA

<sup>5</sup>NASA/GSFC, Greenbelt MD

<sup>6</sup>Hyttec, Inc., Los Alamos, NM

## Abstract

We describe the design, construction and performance of the CsI hodoscopic calorimeter of the GLAST beam test engineering module (BTEM), a full size prototype of one of the 16 towers of the GLAST Large Area Telescope (LAT), approved by NASA to be launched in 2005. The calorimeter is comprised of 80 CsI crystals organized in a hodoscopic arrangement with 8 layers of 10 crystals. The crystals are read out with PIN photodiodes at both ends. Light tapering along the length of the crystals produces an asymmetry in the light measured at the ends. The asymmetry is used for interaction positioning along the length of each crystal. The major design goals included the demonstration of a mechanical design to survive launch into space with minimal passive material, low power electronics with a dynamic range of  $\sim 3 \times 10^5$ , and digital data acquisition with  $< 20 \mu\text{sec}$  dead time per event. We will describe the design and will give results from the analysis of the beam test in winter 1999/2000 at SLAC, where the BTEM was tested in gamma, positron and hadron beams.

## I. INTRODUCTION

GLAST is a next generation high-energy gamma-ray observatory designed for making observations of celestial gamma-ray sources in the energy band extending from 10 MeV to more than 100 GeV. It follows in the footsteps of the Compton Gamma Ray Observatory EGRET experiment, which was operational between 1991-1999. The GLAST Mission is part of NASA's Office of Space and Science Strategic Plan, with launch anticipated in 2005. The principal instrument of the GLAST mission is the Large Area Telescope (LAT) that is being developed jointly by NASA and the US Dept. of Energy (DOE) and is supported by an international collaboration of 26 institutions lead by Stanford University.

The GLAST LAT [1, 2, 3] is a high-energy pair conversion telescope that has been under development for over 7 years with support from NASA and DOE. It consists of a precision converter-tracker, CsI hodoscopic calorimeter, plastic scintillator anticoincidence system and a data acquisition

system. The design is modular with a  $4 \times 4$  array of identical tracker and calorimeter modules. The modules are  $\sim 38 \times 38$  cm.

The primary tasks of the GLAST calorimeter are to provide an accurate measure of the energy of the shower resulting from pair conversion of incident gamma rays in the tracker, and to assist with cosmic-ray background rejection through correlation of tracks in the precision silicon tracker with the position of energy deposition in the calorimeter. Table 1 summarizes the top level GLAST requirements that influence the calorimeter design. The total mass of the GLAST instrument is constrained by the mission's launch vehicle capability. The calorimeter's mass allocation, which was developed as part of the ATD study, is  $\sim 98$  kg per module.

As part of the ATD program we studied a LAT concept that consisted of a  $5 \times 5$  array of 32-cm modules and fabricated a full size prototype module of this design called the beam test engineering model (BTEM). It is the design and test of the BTEM prototype that we report here. As a result of these tests, the configuration of the LAT experiment for the GLAST mission evolved into a more efficient  $4 \times 4$  array of 38-cm modules.

## II. BTEM CALORIMETER DESIGN

The BTEM CsI calorimeter is built on a hodoscopic arrangement of CsI(Tl) scintillation crystals with PIN photodiode readouts. Table 2 summarizes the derived requirements for the calorimeter based on simulations and

Table 1. GLAST Requirements Relevant to the Calorimeter

Parameter	Requirement
Energy Range	20 MeV – 300 GeV
Energy Resolution	10% ( $E > 100$ MeV) goal of 3%
Field of View (FWHM)	$> 2.4$ sr
Effective Area	$> 8,000$ cm <sup>2</sup>
Background Rejection	$> 10^5:1$
Dead Time	$< 20 \mu\text{s}$ per event
Instrument Lifetime	$> 5$ yrs, with no more than 20% degradation.

<sup>1</sup> The development of the GLAST calorimeter is supported by NASA Advanced Technology Development program.

Table 2. Derived Requirements for the Hodoscopic Crystal Calorimeter for the BTEM Prototype.

Parameter	Requirement
Calorimeter Depth	10 radiation lengths ( $X_0$ )
Number of CsI Crystals	80 ( 8 layers of 10)
Crystal Dimensions	$30 \times 23 \times 310$ mm
Number of Electronics Channels:	320 / module (80 CsI blocks, both ends, 2 PIN each)
Dynamic Range:	$5 \times 10^5$ (noise to max signal)
Noise goal:	1 MeV RMS ( $3 \times 10^3 e^-$ )
A to D Range:	$\sim 2$ MeV – 100 GeV
Trigger Rate: (GLAST mission)	Ave: 5500 Hz Peak: 9000 Hz
Self trigger delay:	$< 1 \mu\text{sec}$
Trigger timing jitter	$< 1 \mu\text{sec}$
Trigger Dead time:	$< 20 \mu\text{sec}$
Power:	5 watts / module (conditioned)
Mass	$\sim 98$ kg/ module

testing that has been part of the GLAST Advanced Technology Development (ATD) program. The BTEM calorimeter module contains 80 crystals of size  $30 \text{ mm} \times 23 \text{ mm} \times 310$  mm. The crystals are individually wrapped for optical isolation, and are arranged horizontally in 8 layers of 10 crystals each. Each layer is aligned  $90^\circ$  with respect to its neighbors, forming an  $x$ - $y$  array. (See Figure 1, for example.)

The scintillation crystals are read out with PIN photodiodes. The spectral response of diodes is well matched with the scintillation spectrum of CsI(Tl), which provides for a large primary signal ( $\sim 4,000$  electrons collected in  $1 \text{ cm}^2$  diode per MeV deposited), with correspondingly small statistical fluctuations and thereby high intrinsic spectral resolution.

PIN photodiodes are mounted on both ends of a crystal and measure the scintillation light from an energy deposition in the crystal that is transmitted to each end. The difference in light levels (the light asymmetry) provides a determination of the position of the energy deposition along the CsI crystal.

Figure 2 shows the asymmetry measurement made in beam

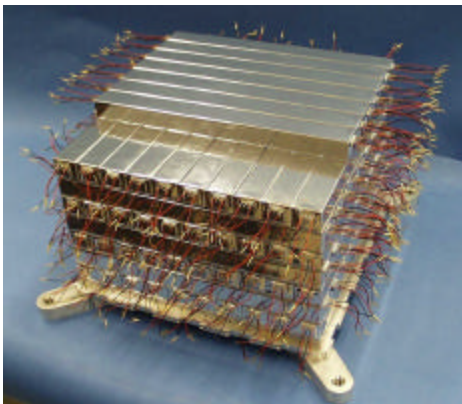


Figure 1. Hodoscopic configuration of CsI crystals in assembly for the BTEM GLAST calorimeter. The crystals are arranged in 8 alternating layers of 10 crystals. PIN photodiodes are mounted on both ends of the CsI crystals.

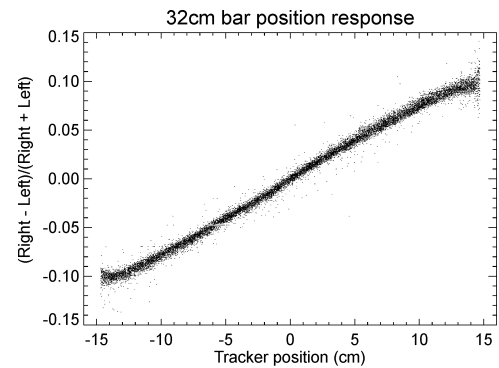


Figure 2. Light asymmetry measurement in a 32-cm crystal measured at SLAC. The calorimeter was mapped with a  $2 \text{ GeV } e^-$  beam which deposited  $\sim 130 \text{ MeV}$  in the crystal.

tests at SLAC. The asymmetry is defined as the difference in the two measurements divided by their sum. The position resolution of this imaging method ranges from a few millimeters for low energy depositions ( $\sim 10 \text{ MeV}$ , see Figure 3) to a fraction of a millimeter for large energy depositions ( $> 1 \text{ GeV}$ ). Improvements in the linearity near the crystal ends were demonstrated in subsequent testing at CERN by modifying the treatment of the ends of the crystals.

## II. ELECTRONICS DESIGN

The major design challenges for the calorimeter electronics are 1) performing spectroscopic measurements over a dynamic range of  $5 \times 10^5$ , 2) keeping power consumption to  $\sim 60$  milliwatts per CsI crystal, including digital readout, and 3) minimizing the processing deadtime to  $\sim 20 \mu\text{sec}$  per event.

The electronics concept addresses the first challenge by dividing the dynamic range into two independent signal chains. The low energy signal covers the energy range from 2 MeV to 800 MeV. The high-energy signal chain covers the range from 40 MeV to 100 GeV. The significant overlap between the two ranges permits cross-calibration of the electronics. A custom PIN photodiode has been developed for GLAST based on the S3590 PIN photodiode from Hamamatsu Photonics. As shown in Figure 4, this custom package mounts two diodes in a single ceramic carrier. The active areas of the two diodes have a ratio of 4 to 1 – the larger area diode covers the low energy band, while the smaller diode covers the high energy band.

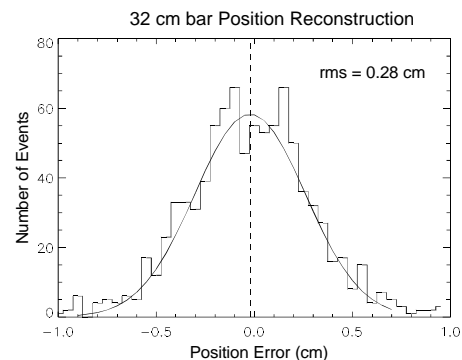


Figure 3. Histogram of positioning errors measured during SLAC beam test at 2 MeV. The  $\sim 130 \text{ MeV}$  deposition in the crystal resulted in positioning error of 2.8 mm (RMS).

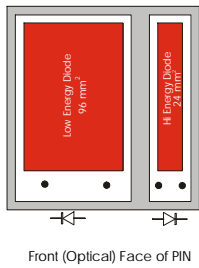


Figure 4. Dual PIN Photodiode Configuration. Active areas of the two diodes have a ratio of 4:1.

Each diode has dedicated preamp and shaping amplifiers that are part of a custom application specific integrated circuit (ASIC). The second challenge of low power consumption per CsI crystal requires the development of a custom CMOS ASIC that is optimized to the performance requirements of the GLAST calorimeter. Even dividing the dynamic range into two separate circuits, the performance specifications for this custom ASIC are significant. For each PIN diode the ASIC contains a preamp, three shaping amps, 4 discriminators, 2 peak-detecting track and holds. The prototype ASIC processes signals from one crystal end – one low energy diode and one high energy diode.

The PIN diode injects charge to a charge sensitive preamp. The sensitivity for the preamps of the low and high energy ranges are different. The preamp signal is further divided into two shaping amps with  $\sim 3.5 \mu\text{sec}$  peaking time. These two shaping amps have gains that differ by  $\times 4$  in the low energy chain ( $\times 8$  in the high energy chain) so that one processes the full dynamic range for that PIN diode, while the other processes only the lowest  $1/4^{\text{th}}$  of the range ( $1/8^{\text{th}}$  in the high energy chain). These two shaping amps are followed by peak-detecting track and holds that capture the peak amplitude of the pulse and stretch it for subsequent digitization by the analog to digital converter (ADC). Reference discriminators on these shaping amps are used by the control electronics to identify the initiation of an event (lower level threshold discriminator) and to identify range overflow.

An additional, faster shaping amplifier with peaking time of  $0.5 \mu\text{sec}$  and associated discriminator is used for calorimeter triggering of the full GLAST instrument.

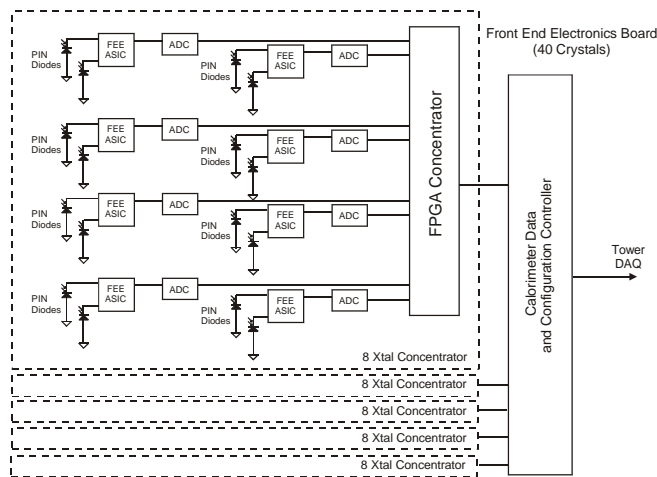


Figure 5. Organization of the Calorimeter Front End Electronics (one of four boards). Each side of the calorimeter is readout in 5 columns of 8 crystals. Data flows to the bottom of the calorimeter for the FPGA concentration. Each crystal end has 2 PIN photodiodes and associated electronics.

Generally, GLAST processing is initiated or triggered by processing of signals in the tracker electronics of each tower. The tracker processing signals the detection of the passage of an  $e^+e^-$  pair through three sequential layers of the tracker. The calorimeter fast shaping discriminator is an alternate trigger mechanism for the instrument and signals the large energy deposition in the calorimeter from gamma rays that did not convert in the tracker or that entered the calorimeter from the side.

To achieve the minimal dead time of the third challenge, commercial, off-the-shelf (COTS) successive approximation analog to digital converters (ADCs) digitize the pulse amplitude signals from the ASIC. Each crystal end has its own ADC so that the required 160 conversions are performed simultaneously. The organization of the readout electronics is shown in Figure 5. Five columnar serial readouts are constructed from the 10 columns of 4 crystals on each side of the calorimeter. Adjacent pairs of columns of 4 crystal ends transfer their data to the bottom of the calorimeter to form one of the six readouts. Field programmable gate arrays (FPGA) merge the serial data from 8 ADCs into a serial message of 128 bits for transfer to the data acquisition system (DAQ). A total of 20 serial communication paths in each tower (5 per side) operate simultaneously to load the data into buffers in the DAQ. In the prototype design the four front end printed circuit boards interface to a controller board that is under the base plate of the calorimeter. This board includes FPGA buffers, command, control, timing and housekeeping functions for the calorimeter-DAQ interface.

### III. MECHANICAL DESIGN

Figure 6 shows the mechanical concept of the BTEM calorimeter developed by Hytec, Inc. The calorimeter module for the prototype is  $10 X_0$  deep constructed with 8 layers of 10 crystals. Crystal dimensions are  $30 \times 23 \times 310 \text{ mm}$ . A compression frame holds the crystals in place against the 10-g Delta II launch loads. The large coefficient of thermal expansion of CsI relative to that of the structural materials of the frame requires that appropriate compliance be designed into the structure to absorb the differential expansion of the CsI over expected temperature range. The design includes 1.6-mm rubber pads between the layers to provide this function. Friction between with CsI wrapping and the

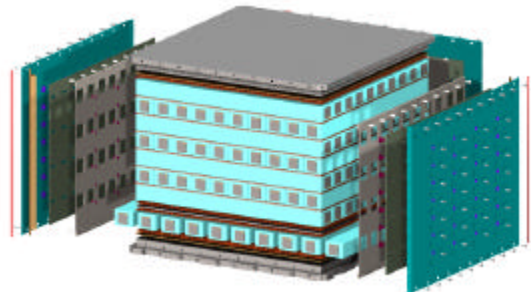


Figure 6. BTEM Calorimeter Design. Eight layers of 10 CsI crystals are held in a compression cell and read out by PIN photodiodes. Four printed circuit cards on the sides support the readout electronics.

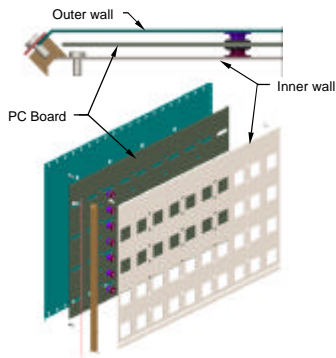


Figure 7. Arrangement of the Printed Circuit Board and Side Closeout of the Compression Cell. The inner wall is the compression cell shear panel and has holes for PIN diode access.

compliant pads hold the CsI crystals against the 3.5-g lateral loads expected on launch.

The vertical compression is held by shear panels that form the inner side walls of the compression cell (see Figure 7). Holes in the shear panels provide access to the PIN photodiodes. Signals from the diodes pass through the panel on flex circuits to the analog front-end electronics printed circuit boards, which attach to the shear panel on each side of the calorimeter. As seen in Figure 7, a final panel is attached to the sides of the compression cell, which provides an electromagnetic shield but also, in combination with the shear panel, forms a stiff structure for lateral loads. Signals from the front-end electronics will travel down to the base of the boards and connect to a data acquisition controller board located under the base compression panel of the calorimeter. That controller will interface with the GLAST data acquisition system (DAQ) for each tower.

#### IV. ASSEMBLY AND TEST

##### A. CsI Crystal Fabrication and Testing

We received and tested 90 CsI crystals, 40 from Crismatec and 50 from Amcrys-H (ISC Kharkov). Crystals from Crismatec were wrapped in heavy Tetratek and had been surface-treated to provide attenuation of scintillation light from end to end. Crystals from Amcrys-H were wrapped in Tyvek and aluminum foil and were polished on all surfaces. The light attenuation treatment for the Amcrys-H crystals was applied at NRL. After characterization of mechanical properties and light yield, custom PIN photodiodes were glued to the end faces of each crystal with Epotek 301. The crystals were then rewrapped with Tetratek and aluminized Mylar. (See Figure 8.)

Final testing of the crystals was performed with cosmic muons. After crystal assemblies were completed we stacked the crystals in a hodoscopic configuration 20 at a time, in two layers of ten crystals. We placed this stack between two-dimensional multiwire proportional counters to form an imaging muon telescope. Signals from the large and small PIN diodes were amplified with low-noise hybrid preamps, and then shaped, digitized, and logged with a CAMAC data acquisition system. For each set of 20 crystals, we collected at

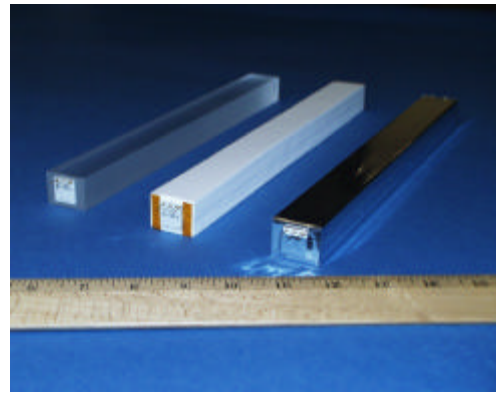


Figure 8. Processing of CsI crystals. After acceptance testing in temporary wrap, PIN diodes are glued on the ends and then final wraps of Tetratek and aluminized Mylar are applied.

least  $10^6$  cosmic muons in both the large and small PIN diodes to characterize the average scintillation light yield in each bar, and to map the light yield as a function of position.

##### B. Scintillation Light Yield

We measured the absolute light yield – in terms of the number of electrons in the Si photodiodes per MeV deposited energy in CsI – by comparing the signal observed from cosmic ray muons, with their known energy deposition, to known charges injected into the test input of the hybrid lab preamp and by direct energy deposition in the Si diode from an  $^{241}\text{Am}$  radioactive source.

Muon data were collected from all 30x23x310 mm crystals for the BTEM calorimeter with a trigger generated by coincidence between two 500 mm square wire chambers. The 23mm dimension of the crystals was vertical. For a typical muon angle-of-incidence of 20 deg, a minimum-ionizing muon gives a typical energy deposition of 13 MeV. We conclude that with 3.5  $\mu\text{s}$  shaping time, the yield is  $\sim 4200$  e/MeV in the 1-cm<sup>2</sup> photodiode and  $\sim 1000$  e/MeV in the  $\frac{1}{4}$ -cm<sup>2</sup> photodiode. Thus the relative light yield in the large and small diodes is indeed equal to their relative geometric area.

Figure 9 shows the distribution of muon light yields in the two PIN diodes for the 80 crystals chosen for the BTEM calorimeter. The rms of the light yield in the large PIN is  $\sim 4\%$ , and the Amcrys crystals are indistinguishable from those

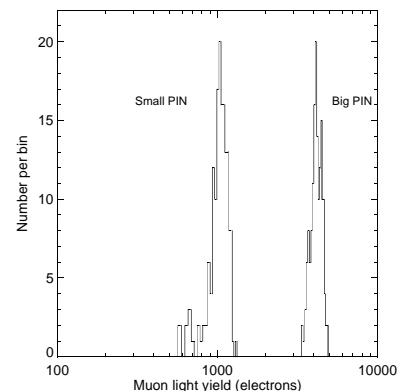


Figure 9. Distribution of light yields for the 80 CsI crystals measured by the big and small PIN diodes. Absolute light yields were scaled from a sample of 13 of the crystals.

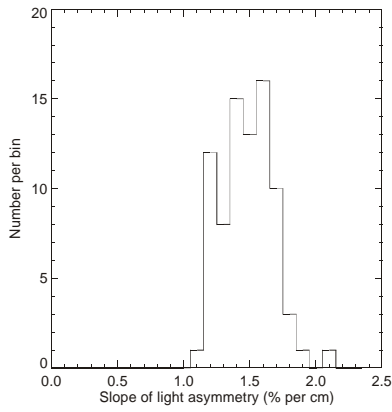


Figure 10. Distribution of measured light asymmetry slopes for the 80 CsI crystals.

from Crismatec.

The rms light yield in the small PIN is ~5%, and there is a small tail extending to low yields that arises from poorer-than-average Epotek bonds in some small PINs. These poorer bonds were not detected in the bench tests with  $^{228}\text{Th}$  that followed the bonding procedure because the 2.7 MeV photopeak was not visible in the small PINs.

### C. Light Asymmetry

From the light asymmetry, i.e. the difference in scintillation light measured at opposite ends of a crystal, we will deduce the crossing point of  $\gamma$ -ray and particle showers for background rejection and calorimeter-only imaging. The light asymmetry as a function of position must be mapped prior to flight, and the mapping will be repeated on orbit with galactic cosmic rays.

Using the muon telescope and crystal stack for interaction position, we calculated the light asymmetry,  $x = (R - L) / (R + L)$ , where R is the signal from the “right” PIN diode and L is the signal from the “left” diode, from the ensemble of cosmic muons collected for both the large and small PINs. For most of the length of a crystal, the asymmetry is linearly related to the position of interaction and, therefore, it is the slope of the asymmetry (expressed e.g. in % per cm) that determines the position resolution of the crystal assembly. To ensure that all crystals would perform adequately for the beam test, we calculated the slope of the light asymmetry in the central 24 cm of each crystal. Figure 10 shows the distribution of light asymmetries of the 80 crystals of the BTEM calorimeter.

### D. Electronics Assembly and Test

The analog ASIC, CSICAL, for the calorimeter was developed by NASA/GSFC using the Orbit 1.2  $\mu\text{m}$  process. The ASIC supports the two PIN photodiodes on one CsI crystal end. It has two preamps, 1 for each diode. Each preamp has three shaping amps - full range at 3.5  $\mu\text{sec}$  shape, 1/4 range (or 1/8 range) at 3.5  $\mu\text{sec}$  shape, and ~ full range at 0.5  $\mu\text{sec}$  shape. It also contains 10 discriminators total, 4 lower level discriminators (LLD) and 6 upper level discriminators (ULD).

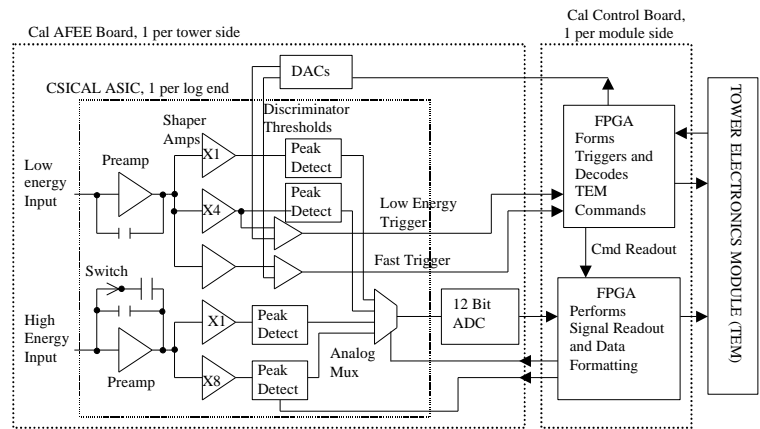


Figure 11. Block diagram for the organization of the BTEM calorimeter electronics. Each of the four AFEE board supports 40 CSICAL ASICs and associated ADCs. There is a Cal controller board for each AFEE board.

There are 4 peak-detecting track and holds – one for each 3.5  $\mu\text{sec}$  shaper (none on 0.5  $\mu\text{sec}$  shaper). A multiplexer on the output of the four track and holds selects the energy range that will be digitized. Digital control signals provide the timing and sequencing for the capture of the event and the subsequent timing for the interface to the ADCs. These control signals are single-ended current controls. A second ASIC, VICAL, converts CMOS voltage control signals into the required current controls. It also converts CSICAL discriminator outputs – current signals into CMOS voltage signals.

Both ASICs were packaged in 44-pin quad flat packs. The packaged ASICs were individually tested at GSFC for functionality and integral linearity. The tested ASICs were then delivered to NRL for installation on the analog front end boards.

The front end electronics design consists of four Calorimeter analog front end electronics (AFEE) circuit boards per tower, each with an accompanying Calorimeter Control board. Figure 11 is a diagram showing the main signal paths in the design. The Cal AFEE board consists of 1) 40 CSICAL ASIC chips, one per log end, 2) 40 Analog to Digital Converter (ADC) chips – one per log end, 3) 10 VICAL ASIC chips, which interface the CSICAL control lines (VICAL ASIC not shown in diagram), 4) 16 Digital to Analog Converters (DACs) for setting bias points and discriminator levels, and 5) other biasing elements.

Figure 13 shows the placement of the AFEE boards on the sides of the calorimeter. The PIN diodes are connected to the cards with test wire loops during initial testing. The AFEE boards interface to the controller boards mounted below the calorimeter.

The control board is the digital interface between the TEM and the AFEE boards. It decode commands from the Tower Electronics Module (TEM), forms trigger requests from either the low energy or fast low energy triggers of selected log ends, counts singles rates in the crystals, and controls acquisition and readout of the ADC energy measurements.

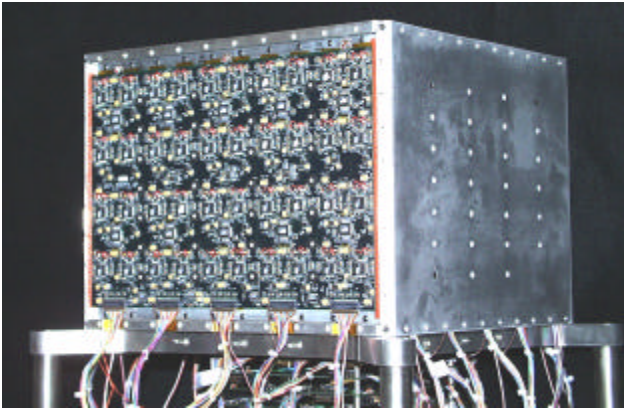


Figure 13. Photo of partially assembled calorimeter with one AFEE card exposed. EMI closeout has been installed on other visible side. cards.

## V. CALIBRATION AND PERFORMANCE

The completed calorimeter module is shown in Figure 12. EMI shield covers the calorimeter controller cards mounted below. The visible cable attaches the calorimeter to the data acquisition system, called the Tower Electronics Module (TEM). Stanford University provided a VME-based PowerPC TEM and a VME-based calorimeter interface circuit card that provided command control and data acquisition for the calorimeter. The TEM runs the VxWorks operating system and communicates with the data acquisition and archiving ground support equipment (GSE) using TCP/IP.

For each received event trigger, the calorimeter digitizes and reads out the 160 signals from the two ends of the 80 CsI crystals. These measurements are formatted into a message of 336 bytes that is transmitted on the TCP/IP event socket. Depending on operating mode, all four energy ranges are readout for each trigger, so that a total of 640 measurements are transmitted for each event.

A PC-based test system was developed for the calorimeter operation, test and calibration. The test system, CalGSE, provided commanding, archiving, data display, housekeeping display and histogramming. Figure 14 shows an example of the CalGSE event display. The display is organized into two halves; the left half displays the four layers of the calorimeter aligned in the X coordinate – the X layers – and the right half displays the four Y layers. The X and Y layer displays are organized into ten columns representing the 10 crystals per layer. The energy deposition (ADC value) in each crystal is color-coded using the scale as indicated. This event is a muon track in the calorimeter as measured in the lowest energy range (LEX4).

Figure 15 shows an event display during the December

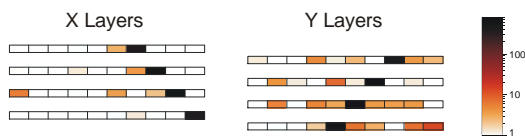


Figure 14. Calorimeter event display shows the response of each crystal. The energy measured in each crystal is color coded as indicated on the right. This event is a muon track in the lowest energy range.



Figure 12. Photo of completed beam test calorimeter suspended on its lifting harness. The mounting plate below is part of the shipping container.

1999 beam test. All four energy ranges are displayed, starting with the lowest energy range (LEX4) on the top and ending with the highest energy range (HE) on the bottom. The display is the result of a beam pulse of  $\sim 15$  positrons, each with an energy of 20 GeV.

Figure 16 shows a CalGSE histogram display from the December, 1999 beam test. The test conditions were the same as those shown in Figure 15 – 20 GeV positrons were incident on the calorimeter with the beam intensity adjusted to approximately 15 positrons (average) per beam pulse. In the bottom right of Figure 16, the multiple peaks in the display are the result of the variation in the number of positrons received in the pulses. In this run, the calorimeter was self-triggering with a discriminator threshold that was sensitive to cosmic

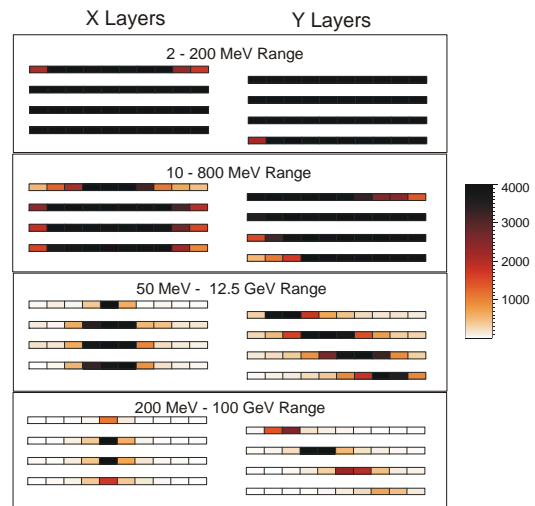


Figure 15. Calorimeter event display shows the response of each crystal in all four energy ranges. The energy measured in each crystal is color coded as indicated on the right. This event was captured during the December beam test and shows the deposition of  $\sim 300$  GeV in the calorimeter from a multi-positron electromagnetic shower.

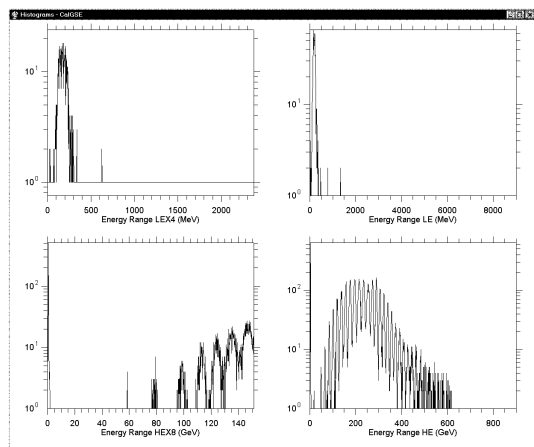


Figure 16. CalGSE histogram display of total energy loss in the calorimeter for each energy range. This run, during the beam test, used 20 GeV positrons. Approximately 15 positrons per beam pulse were observed.

muons. Thus, in the upper left of the figure – the lowest energy range – is the response to muon-only depositions. The energy width of the muon response is due to the variation in muon path lengths through the calorimeter and is not indicative of calorimeter energy resolution.

Using the sampling of the shower profile provided by the segmentation of the calorimeter, one can improve the measurement of the incident energy by correcting for the leakage of the shower from the back of the calorimeter. Two techniques have been studied:

- 1) Fitting the profile of the captured energy to an analytical description of the energy-dependent mean longitudinal profile. This shower profile is reasonably well described by a gamma distribution that is a function only of the location of the shower starting point and the incident energy.
- 2) Correlation of the energy measured in the last layer of the calorimeter with the total energy collected in the calorimeter. Using simulations to calibrate this correlation as a function of energy and incident angle, our French collaborators have found improved resolution in certain energy ranges over profile fitting.

Figure 17 shows the histogram of the measured energy loss in the calorimeter for 20 GeV electrons. The leakage-corrected distribution is also shown. The resultant energy resolution is ~4% (RMS).

## VI. CONCLUSIONS

As a result of the Advanced Technology Development program for GLAST we have demonstrated solutions to all technology challenges associated with the performance of the GLAST LAT calorimeter. The fabrication and test of a full size prototype has provided excellent experience for the development, fabrication and test of the flight instrument.

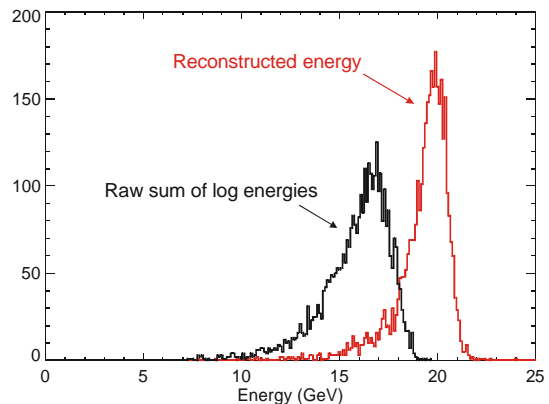


Figure 17. Energy resolution improvement with shower leakage corrections. The histogram of measured total energy in the calorimeter from a beam of 20 GeV positrons shows the effects of shower leakage and improvement with corrections.

In the development of the flight instrument for the GLAST mission, the calorimeter team has been expanded to include collaborators in France and Sweden. The calorimeter development will be a collaboration among the Naval Research Laboratory (NRL), Commissariat à l'Energie Atomique / Département d'Astrophysique, de physique des Particules, de physique Nucléaire et de l'Instrumentation Associée (CEA/DAPNIA), Centre National de la Recherche Scientifique / Institut National de Physique Nucléaire et de Physique des Particules (CNRS/IN2P3) in France, and the Royal Institute of Technology (KTH) and Stockholm University in Stockholm, Sweden. These collaborators bring significant experience and resources for the support of the GLAST mission.

## VII. ACKNOWLEDGEMENTS

The preparation for and execution of the beam test of the GLAST engineering model required the efforts and cooperation of the entire GLAST collaboration. We specifically acknowledge the leadership and support of the Stanford Linear Accelerator Center that made the test possible.

## VIII. REFERENCES

- [1] Michelson, P. E., "GLAST: A detector for high-energy gamma rays", SPIE Conference on Gamma-Rays and Cosmic-Ray Detectors, Techniques, and Missions, August 1996, Denver, CO, (ed: B.D. Ramsey, T. A. Parnell), Vol 2806, p 31
- [2] Johnson, W. N., et al., "A CsI(Tl) Hodoscopic Calorimeter for the GLAST Mission", Nov 1997, IEEE Nuclear Science Symposium, N03-2.
- [3] Atwood, W. B., et al., "Beam test of gamma-ray large area space telescope components", NIM A, vol. 446, pp 444-460, 2000